FISFVIFR

Contents lists available at ScienceDirect

## **Atmospheric Environment**

journal homepage: www.elsevier.com/locate/atmosenv



# Sensitivity and uncertainty analysis of the mechanism of gas-phase chlorine production from NaCl aerosols in the MAGIC model

Paul Nissenson <sup>a</sup>, Jennie L. Thomas <sup>b</sup>, Barbara J. Finlayson-Pitts <sup>b</sup>, Donald Dabdub <sup>a,\*</sup>

#### ARTICLE INFO

Article history: Received 24 September 2007 Received in revised form 25 March 2008 Accepted 26 April 2008

Keywords: Interface chemistry Sea-salt aerosol Sensitivity analysis Chlorine chemistry

## ABSTRACT

This paper presents a global sensitivity and uncertainty analyses of the chlorine chemistry included in the Model of Aqueous, Gaseous and Interfacial Chemistry (MAGIC). Uncertainty ranges are established for input parameters (e.g. chemical rate constants, Henry's law constants, etc.) and are used in conjunction with Latin hypercube sampling and multiple linear regression to conduct a sensitivity analysis which determines the correlation between each input parameter and the model output. The contribution of each input parameter to the uncertainty in the model output is calculated by combining the results of the sensitivity analysis with the input parameters' uncertainty ranges. The peak concentration of molecular chlorine, [Cl<sub>2(g)</sub>]<sub>peak</sub>, is used to compare model runs since MAGIC has demonstrated previously the importance of an interfacial reaction between OH(g) and Cl<sup>-</sup>(aq,surface) in the production of Cl<sub>2(g)</sub>. Results indicate that the interface reaction rate is most strongly correlated with  $\left[\text{Cl}_{2(g)}\right]_{peak}$  and is most responsible for the uncertainty in MAGIC's ability to calculate precisely [Cl<sub>2(g)</sub>]<sub>peak</sub>. In addition, the mass accommodation coefficient for OH and the aqueous-phase reaction rate for  $Cl_2 + OH^- \rightarrow HOCl + Cl^-$  and  $2CO_3^- + O_2 + 2H_2O \rightarrow 2CO_2 \cdot H_2O + 2O_2^-$  also contribute significantly to the uncertainty in  $[Cl_{2(g)}]_{peak}$ .

© 2008 Elsevier Ltd. All rights reserved.

#### 1. Introduction

Field, laboratory and computational studies have shown enhanced production of molecular chlorine from NaCl aerosols (Keene et al., 1993; Pszenny et al., 1993; Hu et al., 1995; Oum et al., 1998; Spicer et al., 1998; Knipping et al., 2000; Knipping and Dabdub, 2002; Finley and Saltzman, 2006), consistent with measured depletions of chloride (and bromide) ions in airborne sea-salt particles (Newberg et al., 2005). Spicer et al. (1998) measured Cl<sub>2(g)</sub> in the marine boundary layer at concentrations higher than expected from known gas- and aqueous-phase chemistry. Aerosol chamber experiments by Oum et al.

E-mail address: ddabdub@uci.edu (D. Dabdub).

(1998) showed that  $Cl_{2(g)}$  is produced from the photolysis of ozone in the presence of water vapor and deliquesced sea-salt particles. Similar results were reported by Knipping et al. (2000) and a surface reaction between Cl<sup>-</sup><sub>(aq.sur-</sub> face) and OH(g) was proposed as an explanation. Knipping et al. (2000) simulated chamber experiments by using a computational model called the Model of Aqueous, Gaseous and Interfacial Chemistry (MAGIC). A detailed description of MAGIC is presented elsewhere (Knipping et al., 2000; Knipping and Dabdub, 2002; Hunt et al., 2004; Thomas et al., 2006). MAGIC significantly underpredicts the concentration of  $\text{\rm Cl}_{2(g)}$  when only considering traditional gas- and aqueous-phase chemistry (Knipping et al., 2000; Knipping and Dabdub, 2002; Thomas et al., 2006). Experimental measurements are reproduced if the following interfacial reaction is included

$$OH_{(g)} + Cl_{(aq,surface)}^{-} \rightarrow 0.5Cl_{2(g)} + OH_{(aq)}^{-}$$
 (1)

<sup>&</sup>lt;sup>a</sup> University of California, Irvine, Department of Mechanical and Aerospace Engineering, Irvine, CA 92697-3975, USA

<sup>&</sup>lt;sup>b</sup> University of California, Irvine, Department of Chemistry, Irvine, CA 92697-2025, USA

<sup>\*</sup> Corresponding author. Tel.: +1 (949) 824 6126; fax: +1 (949) 824 8585.

Knipping and Dabdub (2003) showed that including reaction (1) along with some additional chlorine chemistry in a chemical transport model leads to increased ozone production in tropospheric marine regions. This result is consistent with other studies which suggest that  $\text{Cl}_{2(g)}$  in urban air increases ozone concentration (Tanaka et al., 2000). By contrast, halogen chemistry in the polar boundary layer tends to decrease the concentration of ozone at polar sunrise (Foster et al., 2001; Sander, 2007; Simpson et al., 2007; von Glasow and Crutzen, 2007).

A Sensitivity and uncertainty analyses aim to understand which input parameters dominate the production of  $\text{Cl}_{2(g)}$ . This information can direct further research toward examining and refining estimates of these input parameters, allowing reaction (1) to be represented more accurately in chemical transport models.

Varying levels of uncertainty are associated with each rate constant, mass accommodation coefficient and other input parameters which can impact the predicted  $\text{Cl}_{2(g)}$  concentrations. However, the complex, non-linear interplay among the physical and chemical processes in MAGIC makes it difficult to ascertain the sensitivity of  $\text{Cl}_{2(g)}$  production to each input parameter. Monte Carlo methods have been applied to chemical mechanisms because they are well-suited for problems with a large number of input parameters and allow for standard statistical tests, such as multiple linear regression, to be applied to the output (Derwent and Høv, 1988; Gao et al., 1996; Phenix et al., 1998; Hanna et al., 2001; Rodriguez and Dabdub, 2003).

This study presents results from a first-order sensitivity and uncertainty analyses of the MAGIC computational model. Uncertainty ranges are established for 197 input parameters from an extensive literature search. A Monte Carlo sampling technique called Latin hypercube sampling is used in conjunction with multiple linear regression to conduct the sensitivity analysis which yields the correlation between the input parameters and model output. The peak concentration of  $Cl_{2(g)}$ ,  $[Cl_{2(g)}]_{peak}$ , is used to compare model runs since MAGIC has demonstrated in previous work the importance of reaction (1) in the production of Cl<sub>2(g)</sub> (Knipping et al., 2000; Knipping and Dabdub, 2002; Thomas et al., 2006). The photolysis of  $Cl_{2(g)}$  produces  $Cl_{(g)}$ , an important oxidant in the atmosphere. If the current knowledge of the production pathways of Cl<sub>2(g)</sub> is improved, ozone formation would be predicted more accurately in air quality models than is currently possible.

The sensitivity analysis gives the strength of the correlation between each input parameter and  $[Cl_{2(g)}]_{peak}$ , but cannot reveal the contribution of each input parameter to the uncertainty in MAGIC's ability to calculate precisely  $[Cl_{2(g)}]_{peak}$ . An uncertainty analysis is conducted to determine this. The uncertainty analysis combines the results from the sensitivity analysis with estimates of the parameters' uncertainty ranges to establish the most influential input parameters on the uncertainty of  $[Cl_{2(g)}]_{peak}$ . Input parameters that contribute significantly to the uncertainty of  $[Cl_{2(g)}]_{peak}$  may be good candidates for further study since a reduction in their uncertainty ranges would reduce the uncertainty of  $[Cl_{2(g)}]_{peak}$  in MAGIC.

The global sensitivity analysis conducted in this study is more rigorous than the local sensitivity analysis used in Knipping and Dabdub (2002). A local sensitivity analysis provides a general sense of which input parameters correlate strongly with  $Cl_{2(g)}$  production. However, a global sensitivity analysis captures the entire interactions in the system. In Knipping and Dabdub (2002), correlation coefficients are calculated by varying the input parameters one at a time by 1% and examining the percent change in  $Cl_{2(g)}$ production. The present work calculates correlation coefficients by varying all input parameters simultaneously over their uncertainty ranges using Latin hypercube sampling. Therefore, the results for the sensitivity analysis in this paper are more realistic than the results presented in Knipping and Dabdub (2002). Although other sensitivity analysis techniques exist, for example a Green's function approach (Vuilleumier et al., 1997), a global sensitivity analysis using Monte Carlo methods is commonly used on chemical models (Derwent and Høv. 1988: Gao et al., 1995; Phenix et al., 1998; Hanna et al., 2001; Rodriguez and Dabdub, 2003). In addition, this work also quantifies the contribution of each input parameter to the uncertainty in  $[Cl_{2(\sigma)}]_{peak}$  which was not performed in Knipping and Dabdub (2002).

## 2. Methodology

## 2.1. Establishing error ranges for input parameters

Almost all of the model input parameters examined in this study are listed in Knipping and Dabdub (2002). This includes 62 gas-phase reaction rate constants, 104 aqueous-phase reaction rate constants, 10 mass accommodation coefficients, 10 Henry's law constants and 9 acid/base equilibrium constants. This study also examines the interface reaction (1) and a weighting factor for the kinetic salt effect (both described below). A table listing the uncertainty ranges for all input parameters that were determined from an extensive literature search is included as Supplementary Material.

The size of the uncertainty ranges varies greatly. For example, the reaction rate constant for the gas-phase reaction  $O(^{1}D) + O_{2} \rightarrow O(^{3}P) + O_{2}$  has a relatively small uncertainty factor of 1.1 (Sander et al., 2006) while the reaction rate constant for the gas-phase reaction  $O(^{3}P)$  +  $HOCl \rightarrow ClO + OH$  has a relatively large uncertainty factor of 3 (Sander et al., 2006). For some input parameters, an uncertainty range was estimated due to a lack of available data. The input parameters that do not have well-established uncertainty ranges fall into the following categories. (i) There exists only one reference in which an input parameter's mean is given and no uncertainty range is reported. For these parameters, an arbitrary uncertainty range is selected, usually  $\pm 50\%$ . This percentage is on par with the other input parameters' uncertainty ranges. (ii) A lone reference reports only an upper or lower limit. For these input parameters, the mean and uncertainty range are established by selecting two points, the limit value reported in the literature and the other extreme value. For example, the upper limit for the reaction rate constant for the gas-phase reaction  $ClO + O_3 \rightarrow OClO + O_2$  is  $k_{298} < 1 \times 10^{-18}~\rm cm^3~molec^{-1}~s^{-1}$  (Sander et al., 2006). The points 0 and  $1 \times 10^{-18}~\rm cm^3~molec^{-1}~s^{-1}$  are used to calculate the mean and standard deviation  $(0.50 \pm 0.50) \times 10^{-18}~\rm cm^3~molec^{-1}~s^{-1}$ . (iii) Two or more references report different values with no uncertainty range. For these parameters, the mean and uncertainty range are calculated using the reported values. The only initial experimental condition varied is the initial gas-phase concentration of CO<sub>2</sub>, which is chosen to determine the impact of dissolved CO<sub>2</sub> on the acid/base equilibrium in the aerosol and the subsequent effect on the uncertainty due to acid/base dependent input parameters.

## 2.1.1. Interface reaction rate

The interface reaction rate, expressed in terms of the aqueous-phase product formed, is defined as (Schwartz, 1986)

$$R_{\rm int} = \left(\frac{r^2}{3D_{\rm g}} + \frac{4r}{3\nu\gamma}\right)^{-1} \left[ OH_{\rm (g)}^{\cdot} \right] \tag{2}$$

where the overall surface reaction probability is

$$\gamma = \phi \gamma' \beta_{\rm Cl} \left[ Cl_{\rm (aq)}^{-} \right], \tag{3}$$

r is the aerosol radius,  $D_{\rm g}$  is the gas-phase diffusion coefficient, v is the mean molecular speed of the colliding gas,  $\beta_{\rm Cl}[{\rm Cl}^-_{\rm (aq)}]$  is the fraction of the droplet surface covered by chloride ions,  $\phi$  is the average number of contacts between  ${\rm OH}_{\rm (g)}$  and surface  ${\rm Cl}^-_{\rm (aq)}$ .  $\gamma'$  denotes the probability that  ${\rm Cl}^-_{\rm (aq)}$  and  ${\rm OH}_{\rm (g)}$  will react when these species come in contact and can theoretically vary from 0 to 1. In this study,  $\gamma'$  is the parameter varied in the interface reaction rate. Laskin et al. (2006) report a lower limit of  $\gamma'=0.2$  (This value is obtained by converting Laskin et al.'s  $\gamma_{\rm net}$  to our  $\gamma'$  and, then dividing by two to account for the uncertainty factor of two in  $\gamma_{\rm net}$ ). Although the other variables within Eqs. (2) and (3) may have a significant uncertainty associated with them, this study only varies  $\gamma'$ , which is allowed to vary from 0.2 to 1.

## 2.1.2. Kinetic salt effect

If a reaction includes two or more ion reactants

$$C + D \rightarrow products$$
 (4)

its rate constant is a function of the ionic strength and the charge on the reactants (Perlmutter-Hayman, 1971; Rochester, 1971; Pethybridge and Prue, 1972). MAGIC uses the Debye–Huckel–Bronsted equation to calculate the kinetic salt effect

$$\log(k) = \log(k^{\circ}) + \left(2z_{\rm C}z_{\rm D}AI^{1/2}\right) / \left(1 + I^{1/2}\right)$$
 (5)

where I is the ionic strength,  $z_{\rm C}$  and  $z_{\rm D}$  are the charges on the reactants, k is the adjusted reaction rate constant including the kinetic salt effect,  $k^{\circ}$  is the reaction rate constant at infinite dilution ( $I=0~{\rm M}$ ) and A is the Debye parameter.

Substituting  $\delta = (2z_C z_D A I^{1/2})/(1 + I^{1/2})$ , Eq. (5) is rewritten as

$$k = k^{\circ} \times 10^{\delta} \tag{6}$$

Eq. (6) works well for  $I \le 0.5$  M (Pethybridge and Prue, 1972). However, the ionic strength of the NaCl aerosols in

the simulations is  $\sim$ 5 M. Therefore, Eq. (6) should be viewed as a rough approximation to the kinetic salt effect and is rewritten as

$$k = k^{\circ} Q(I, \Delta z). \tag{7}$$

Due to uncertainty of the actual value of  $Q(I,\Delta z)$ , this term is varied from 1 (no kinetic salt effect) to the value produced by Eq. (6),  $10^{\delta}$ . The upper limit value is chosen since Eq. (6) is an overestimate of the kinetic salt effect for a NaCl solution (Pethybridge and Prue, 1972). In order to accomplish this, a multiplicative factor ( $\Psi$ ) is introduced into Eq. (6)

$$k = k^{\circ} \times 10^{\Psi \delta} \tag{8}$$

and  $\Psi$  varies from 0 to 1.

#### 2.2. Latin hypercube sampling

Monte Carlo techniques have been used extensively to conduct sensitivity analysis of gas-phase chemical mechanisms (Derwent and Høv, 1988; Gao et al., 1996; Phenix et al., 1998; Hanna et al., 2001; Rodriguez and Dabdub, 2003). In a Monte Carlo analysis, input parameters are treated as random variables that follow a particular probability distribution. In this study, all input parameters are given a log-normal probability distribution with the exception of the kinetic salt effect factor  $(\Psi)$  which is given a uniform probability distribution.

Latin hypercube sampling is a particular form of Monte Carlo sampling and has been described in detail elsewhere (McKay et al., 1979; Derwent and Høv, 1988; Rodriguez and Dabdub, 2003). McKay et al. (1979) demonstrated that Latin hypercube sampling converges to the same solution as regular Monte Carlo sampling, but requires nearly an order of magnitude less simulations. In Latin hypercube sampling, each of the  $N_T$  input parameters ( $N_T = 197$  in this study) are assigned a probability distribution that is a function of its mean and standard deviation. These probability distributions are discretized into n non-overlapping intervals of equal probability and a value of the input parameter is selected at random within each of the intervals. Thus, all input parameters are sampled n times and  $n \times N_T$  total values are selected. For every input parameter, each of the nvalues is assigned randomly to one of *n* simulations. The number of simulations is sufficiently large (n = 5000 in this study) to ensure that the results are independent of the number of simulations.

## 2.3. Multiple linear regression

The model output is analyzed using multiple linear regression to establish the correlation between the input parameters and model output. Although the relationships between the input and output parameters are never exactly linear, the first-order approximation is commonly used (Derwent and Høv, 1988; Gao et al., 1995; Gao et al., 1996; Rodriguez and Dabdub, 2003).

The input parameters varied in this study typically are not expressed as explicit functions of each other and this study assumes that they may be independently varied. The regression model is based on the following relationship

$$(y_{i,j}/y_i^*) = \beta_{i,0} + \sum_{l=1}^{N_T} \beta_{i,l}(x_{l,j}/x_l^*) \ i = 1,...,M; j = 1,...,n$$
 (9)

where  $x_{l,j}$  is the input parameter l for simulation j,  $x_l^*$  is the nominal (mean) value of input parameter l,  $y_{l,j}$  is the output parameter i from simulation j,  $y_i^*$  is the output parameter i using nominal values for the input parameters,  $\beta_{i,0}$  is a constant from the regression analysis and  $\beta_{i,l}$  is the regression coefficient between input parameter l and output parameter i. The regression coefficients quantify the sensitivity of output parameter i to each input parameter l.

#### 2.4. Uncertainty analysis

The regression coefficients from the sensitivity study are combined with the variance of each input parameter to yield a first-order approximation of the contribution of each input parameter l to the uncertainty of output parameter i

$$u_{l,i} = \frac{\left(\sigma_l/x_l^*\right)^2 \left(\beta_{i,l}\right)^2}{\sum_{l=1}^{N_{\rm T}} \left(\sigma_l/x_l^*\right)^2 \left(\beta_{i,l}\right)^2},\tag{10}$$

where  $\sigma_l$  is the standard deviation of input parameter l. Eq. (10) is the same expression used in Rodriguez and Dabdub (2003) and similar to the expression in Gao et al. (1996).

As noted in Section 2.1, it is necessary to construct uncertainty ranges for input parameters whose uncertainty ranges are not well established in the literature. This limitation should not affect the results of the sensitivity analysis significantly since the regression coefficients are derived using multiple linear regression which assumes that the relationship between each input parameter and the model output is linear; changing the uncertainty range should not (in theory) affect significantly the regression coefficients. However, the uncertainty analysis is affected by this limitation because the contribution of each input parameter to the uncertainty in  $[Cl_{2(g)}]_{peak}$  is a function of its standard deviation. Large uncertainty ranges are chosen to ensure an upper limit to the uncertainty associated with these input parameters.

## 2.5. Simulation conditions

MAGIC originally was developed to simulate a series of chamber experiments described in various sources (Knipping et al., 2000; Knipping and Dabdub, 2002). These experiments are used for the present sensitivity analysis because the initial concentrations and conditions were well defined and the gaseous Cl<sub>2</sub> product was measured. The chamber is filled with humidified air, ozone and deliquesced NaCl particles at 298 K. The chamber conditions used in the simulations are described in Table 1. In the simulations, the system is held in the dark for 600 s before irradiation with 254 nm UV lamps in order to reproduce

**Table 1**Model parameters used in the simulations (Knipping and Dabdub, 2002; Thomas et al., 2006)

Model parameter	
Aerosol median diameter (nm)	224
Aerosol geometric standard deviation	1.9
Aerosol concentration	$1.86 \times 10^5$ particles cm <sup>-3</sup>
Relative humidity (%)	82
Temperature (K)	298
[NaCl] <sub>0</sub> (M)	4.3
$[O_3]_0(ppmv)$	1.6
$[CO_{2(g)}]_0$ (ppmv)	1.5 (case 1)
	10 (case 2)
	380 (case 3)
$\beta_{\text{Cl}}$ (M <sup>-1</sup> )	0.02
φ	3

the experimental protocol. The length of the dark interval has no significant impact on the results.

Knipping and Dabdub (2002) note that the initial concentration of  $CO_{2(g)}$  may impact the concentration of  $[CI_{2(g)}]_{peak}$  significantly in the  $[CO_{2(g)}]_0 = 1$ –10 ppmv range since dissolved  $CO_{2(g)}$  acts as an acid, reducing the alkalinity of the aerosols. If no  $CO_2$  is present in the system, the  $CI_{2(aq)}$  loss routes via  $OH_{(aq)}^-$  and  $HO_{2(aq)}^-$  become increasingly significant due to increased pH, and  $CI_{2(g)}$  is greatly reduced. Three sets of simulations are conducted to examine the influence of the initial concentration of  $CO_{2(g)}$  on  $[CI_{2(g)}]_{peak}$ : (1)  $[CO_{2(g)}]_0 = 1.5$  ppmv; (2)  $[CO_{2(g)}]_0 = 10$  ppmv; and (3)  $[CO_{2(g)}]_0 = 380$  ppmv.

In the chamber experiments and simulations conducted for this study, the aerosols have a mean diameter  $(d_{\rm m})$  of 224 nm, which is typical of the peak in the number concentration distribution of marine aerosols (although the mass concentration distribution is dominated by large, micronsized particles as discussed in Fitzgerald, 1991). However, since the surface area to volume ratio goes as  $1/d_{\rm m}$ , it is expected that aqueous-phase chemistry will become more important as  $d_{\rm m}$  increases.

## 3. Results and discussion

## 3.1. Uncertainty in $[Cl_{2(g)}]_{peak}$

Fig. 1 shows the average and 1 standard deviation concentration for  $\text{Cl}_{2(g)}$  as a function or time for the  $[\text{CO}_{2(g)}]_0 = 1.5$  ppmv case. During the first 600 s, the UV lamps are off and there is no production of  $\text{Cl}_{2(g)}$ . At 600 s, the UV lamps are turned on and the production of  $\text{Cl}_{2(g)}$  increases rapidly (initiated by OH formed from ozone photolysis), eventually reaching a peak after several hundred seconds. The mean value of  $[\text{Cl}_{2(g)}]_{\text{peak}}$  is 23 ppbv with a standard deviation of 8 ppbv. Although these values differ somewhat for the  $[\text{CO}_{2(g)}]_0 = 10$  ppmv and  $[\text{CO}_{2(g)}]_0 = 380$  ppmv cases, the  $[\text{Cl}_{2(g)}]$  profiles are qualitatively similar. The mean and standard deviation of  $[\text{Cl}_{2(g)}]_{\text{peak}}$  for the three  $[\text{CO}_{2(g)}]_0$  cases are listed in Table 2.

Knipping and Dabdub (2002) found that  $[CO_{2(g)}]_0$  is an important factor in determining  $[Cl_{2(g)}]_{peak}$  in the range of  $[CO_{2(g)}]_0 = 1-10$  ppmv and that  $[CO_{2(g)}]_0$  becomes less of

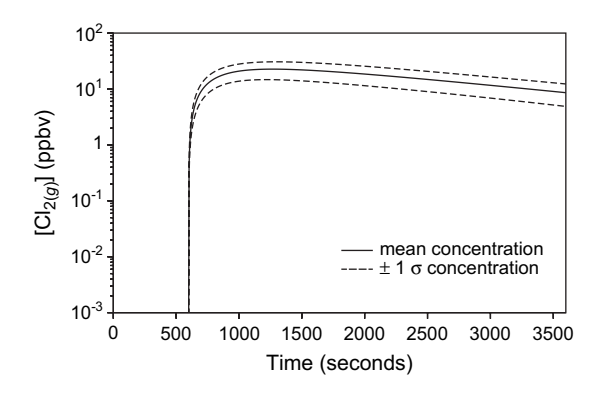


**Fig. 1.** The average (solid line) and 1 standard deviation (dashed line) concentration of  $Cl_{2(g)}$  versus time for the  $[CO_{2(g)}]_0 = 1.5$  ppmv scenario. At 600 s, the UV lamps are turned on and  $Cl_{2(g)}$  production increases rapidly. The mean value of  $[Cl_{2(g)}]_{peak}$  is 23 ppbv with a standard deviation of 8 ppbv.

a factor at higher concentrations. Results in Table 2 are consistent with that finding as the mean value of  $[\mathrm{Cl}_{2(g)}]_{peak}$  increases by 26% when  $[\mathrm{CO}_{2(g)}]_0$  is increased from 1.5 ppmv to 10 ppmv, but only increases another 17% from 10 ppmv to 380 ppmv. As  $[\mathrm{CO}_{2(g)}]_0$  increases, more  $\mathrm{CO}_{2(g)}$  is taken up into the aerosols and upon reaction with water forms  $\mathrm{HCO}_{3(aq)}^-$  and  $\mathrm{H}_{(aq)}^+$ , decreasing the pH of the aerosols (Fig. 2). This decrease in pH reduces  $\mathrm{Cl}_{2(aq)}$  loss via reactions with  $\mathrm{OH}_{(aq)}^-$  and  $\mathrm{HO}_{2(aq)}^-$ , which favors increased  $[\mathrm{Cl}_{2(g)}]$ .

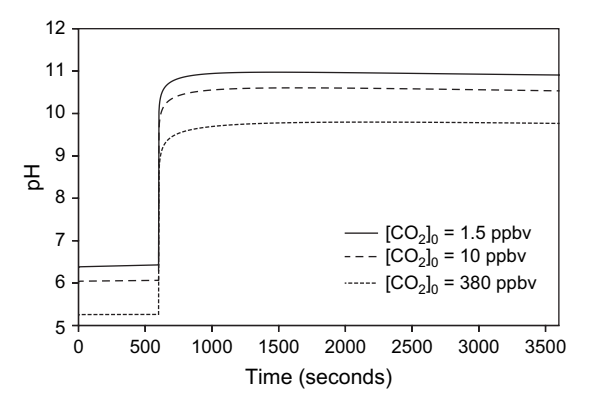


**Fig. 2.** Average droplet pH versus time for each  $[CO_{2(g)}]_0$  case.

## 3.2. Sensitivity and uncertainty analyses

Results of the sensitivity and uncertainty analyses are presented together for clarity since the sensitivity analysis directly impacts the uncertainty analysis. Table 2 lists the input parameters that have the strongest correlation with  $[\operatorname{Cl}_{2(g)}]_{\text{peak}}$ , contribute the most to the uncertainty in  $[\operatorname{Cl}_{2(g)}]_{\text{peak}}$  or are otherwise interesting. Input parameters with either a regression coefficient ( $\beta_{i,l}$  from Eq. (9)) greater than 0.1 and/or contribute more than 1% to the total uncertainty in  $[\operatorname{Cl}_{2(g)}]_{\text{peak}}$  for any of the three  $[\operatorname{CO}_{2(g)}]_0$  cases are included in Table 2.

Table 2 Results from sensitivity and uncertainty analyses for all three  $[CO_{2(g)}]_0$  cases

$[\operatorname{Cl}_{2(g)}]_{\operatorname{peak}}(\mu \pm \sigma)$ Parameter <sup>a</sup>		Case 1: $[CO_{2(g)}]_0 = 1.5 \text{ ppmv}$ $23 \pm 8 \text{ ppbv}$		Case 2: $[CO_{2(g)}]_0 = 10 \text{ ppmv}$ $29 \pm 10 \text{ ppbv}$		Case 3: $[CO_{2(g)}]_0 = 380 \text{ ppmv}$ $34 \pm 12 \text{ ppbv}$	
	$\sigma/\mu$						
		β	u (%)	β	u (%)	β	и (%)
Interface reaction rate parameter							
$\gamma'$ (reaction probability)	0.67	+0.62	73.3	+0.62	77.5	+0.63	75.7
Gas-phase reaction rate constants							
$O_3 + hv \rightarrow O(^1D) + O_2$	0.15	+0.52	2.6	+0.46	2.2	+0.41	1.6
$O(^{1}D) + H_{2}O \rightarrow 2OH$	0.14	+0.44	1.6	+0.42	1.5	+0.35	1.0
$O(^{1}D) + N_{2} \rightarrow O(^{3}P) + N_{2}$	0.10	-0.35	0.5	-0.30	0.4	-0.23	0.2
$O_3 + OH \rightarrow HO_2 + O_2$	0.18	-0.31	1.3	-0.30	1.4	-0.29	1.2
$H_2O_2 + OH \rightarrow HO_2 + H_2O$	0.23	N/C	N/C	-0.02	0.0	-0.16	0.6
Aqueous-phase reaction rate constants							
$Cl_2 + OH^- \rightarrow HOCl + Cl^-$	0.67	-0.24	10.7	-0.21	8.8	-0.14	3.7
$HCO_3^- + O_2^- \rightarrow CO_3^- + HO_2^-$	0.33	N/C	N/C	-0.03	0.0	-0.14	0.9
$CO_3^- + HO_2^- \rightarrow CO_3^{2-} + HO_2$	0.59	N/C	N/C	+0.01	0.0	+0.10	1.6
$CO_3^- + O_2^- \to CO_3^{2-} + O_2$	0.40	N/C	N/C	+0.01	0.0	+0.14	1.4
$2CO_3^- + O_2 + 2H_2O \rightarrow 2CO_2 \cdot H_2O + 2O_2^-$	0.86	N/C	N/C	-0.02	0.1	-0.14	6.3
Mass accommodation coefficients							
$\alpha(OH)$	0.98	-0.10	4.1	-0.09	4.0	-0.07	1.8
Henry's law constant							
$H(Cl_2)$	0.17	-0.51	3.2	-0.43	2.3	-0.26	0.9
Acid/base equilibrium constants ( $K_{eq}$ )							
$H_2O \leftrightarrow OH^- + H^+$	0.12	-0.26	0.4	-0.21	0.4	-0.15	0.1
$CO_2 \cdot H_2O \leftrightarrow HCO_3^- + H^+$	0.20	+0.13	0.3	+0.10	0.2	-0.04	0.0
$HCO_3^- \leftrightarrow CO_3^{2-} + H^+$	0.12	+0.14	0.1	+0.12	0.1	+0.06	0.0
Kinetic salt effect parameter							
$\Psi$	1.0	N/C	N/C	N/C	N/C	-0.02	0.2

N/C: the correlation between the input parameter and  $[Cl_{2(g)}]_{peak}$  is not statistically significant.

<sup>&</sup>lt;sup>a</sup> No other input parameters have a regression coefficient larger than 0.1 or contribute more than 1% to the uncertainty in  $[Cl_{2(g)}]_{peak}$ .

The correlation between  $[\mathrm{Cl}_{2(g)}]_{peak}$  and each of the 197 input parameters is calculated by applying Eq. (9) to the simulation output. Note that if an input parameter is correlated weakly with  $[\mathrm{Cl}_{2(g)}]_{peak}$  it may be correlated strongly with other output parameters (e.g. droplet pH, concentrations of reaction products, etc.). The contribution of each input parameter to the uncertainty of  $[\mathrm{Cl}_{2(g)}]_{peak}$  is calculated using Eq. (10). As with the sensitivity analysis, if an input parameter contributes little to the uncertainty in  $[\mathrm{Cl}_{2(g)}]_{peak}$ , it may contribute significantly to the uncertainty in other output parameters.

The major goal of this study is to identify which input parameters contribute the most to model uncertainty, which is calculated from Eq. (10). The results of the uncertainty analysis also suggest priorities for refining uncertainty ranges of the input parameters. Prime candidates for further study are those input parameters that both contribute significantly to the uncertainty of  $[Cl_{2(g)}]_{peak}$  and have a relatively large uncertainty range. It may be easier to narrow these parameters' relatively large uncertainty ranges (and therefore reduce the uncertainty in  $[Cl_{2(g)}]_{peak}$ ) compared to those input parameters with small uncertainty ranges.

## 3.2.1. Interface reaction rate

In all three  $[CO_{2(g)}]_0$  cases, the interface reaction rate (specifically  $\gamma'$ ) correlates strongly with  $[Cl_{2(g)}]_{peak}$ . The large, positive correlation is expected since this reaction is primarily responsible for the production of  $Cl_{2(g)}$  (Knipping and Dabdub, 2002). Approximately 75% of the uncertainty in  $[Cl_{2(g)}]_{peak}$  is attributed to this input parameter and it has a relatively large uncertainty range. The ability of MAGIC to calculate  $[Cl_{2(g)}]_{peak}$  could be greatly improved if the interface reaction probability were more precisely known.

#### 3.2.2. Gas-phase reaction rate constants

There are five gas-phase reaction rate constants that are strongly correlated with  $[Cl_{2(g)}]_{peak}$ . These reactions are responsible for either the production or destruction of  $OH_{(g)}$  (directly or indirectly) which is the oxidant in reaction (1). The reactions that lead to  $OH_{(g)}$  production correlate positively with  $[Cl_{2(g)}]_{peak}$  while the reactions that lead to  $OH_{(g)}$  destruction correlate negatively with  $[Cl_{2(g)}]_{peak}$ . Although these gas-phase reaction rate constants have large regression coefficients, their uncertainty ranges are relatively narrow and therefore contribute only  $\sim 5-7\%$ (combined) to the uncertainty of  $[Cl_{2(g)}]_{peak}$ . Any effort to decrease the uncertainty ranges of these input parameters would improve only marginally MAGIC's ability to calculate  $[Cl_{2(g)}]_{peak}$  precisely. In addition, the rate of O<sub>3</sub> photolysis is dependent upon experimental conditions and the method of measuring the photolysis rate. Therefore this study recommends that accurate photolysis rate measurements (or estimates in the case of air quality modeling) be used when modeling sea-salt aerosol chemistry.

#### 3.2.3. Aqueous-phase reaction rate constants

The aqueous-phase reaction rate constant for  $Cl_{2(aq)} + OH_{(aq)}^- \to HOCl_{(aq)} + Cl_{(aq)}^-$  (reaction 138) is correlated most strongly with  $[Cl_{2(g)}]_{peak}$  out of all aqueous-phase

reaction rate constants. This reaction destroys  $Cl_{2(aq)}$ , increasing the gradient between gas- and aqueous-phase  $Cl_2$  and forcing more  $Cl_{2(g)}$  to diffuse into the aerosols. Therefore, this reaction rate constant is correlated negatively with  $[Cl_{2(g)}]_{peak}$ . Since this parameter is a significant contributor to the uncertainty of  $[Cl_{2(g)}]_{peak}$  for all three  $[CO_{2(g)}]_0$  cases ( $\sim$ 4–10% depending on pH) and its uncertainty range is relatively large, it is a good candidate for further study.

Aqueous-phase reactions involving carbonate chemistry become significant at higher initial concentrations of  $CO_{2(g)}$ . As  $[CO_{2(g)}]_0$  is increased, the aerosol pH decreases and the concentration of the carbonate radical anion  $(CO_{3(aq)}^{-})$  increases. Reactions between  $CO_{3(aq)}^{-}$  and species that affect the aerosol pH, such as  $O_{2(aq)}^{-}$  and  $HO_{2(aq)}^{-}$  (via reaction 70, 72, 77, 78, 87, 88 and 90), become increasingly important because OH<sup>-</sup>(aq) destroys Cl<sub>2(aq)</sub> (reaction 138). In addition,  $O_{2(aq)}^{-}$  and  $HO_{2(aq)}^{-}$  can destroy  $Cl_{2(aq)}^{-}$  (reaction 124) and  $Cl_{2(aq)}$  (reaction 141) directly. These carbonate radical anion reactions contribute significantly (~8%) to the uncertainty of  $[Cl_{2(g)}]_{peak}$  at atmospherically relevant concentrations of carbon dioxide. Based on the uncertainty analysis, of all the aqueous-phase reactions involving carbonate ion chemistry, the rate constant for 2CO<sub>3</sub>(aq) +  $O_{2(aq)} + 2H_2O_{(aq)} \rightarrow 2CO_2 \cdot H_2O_{(aq)} + 2O_{2(aq)}^-$  is the most important for further study (at high  $CO_{2(g)}$  concentrations) since its uncertainty range is large.

## 3.2.4. Mass accommodation coefficients

The mass accommodation coefficient  $(\alpha)$  is the probability that a gas-phase molecule will be taken up into a liquid once it reaches the surface. This input parameter has the largest regression coefficient of all mass accommodation coefficients. As  $\alpha(OH)$  increases, less  $OH_{(g)}$  is available to react with  $Cl^-_{(aq,surface)}$  and less  $Cl_{2(g)}$  is produced via reaction (1). Therefore,  $\alpha(OH)$  is negatively correlated with  $[Cl_{2(g)}]_{peak}$ .  $\alpha(OH)$  has a large uncertainty range and contributes  $\sim 2-4\%$  to the uncertainty of  $[Cl_{2(g)}]_{peak}$ . making this input parameter a good candidate for further measurements.

## 3.2.5. Henry's law constants

The Henry's law constant (H) is defined as the ratio of a species' aqueous-phase concentration to its gas-phase concentration at equilibrium. While  $[\operatorname{Cl}_{2(g)}]_{peak}$  has a strong negative correlation with the  $H(\operatorname{Cl}_2)$ , the uncertainty range for this input parameter is relatively narrow; hence, its contribution to the uncertainty in  $[\operatorname{Cl}_{2(g)}]_{peak}$  is relatively small.

## 3.2.6. Acid/base equilibrium constants

There are a few acid/base equilibrium constants that are significantly correlated with  $[Cl_{2(g)}]_{peak}$ . However, these parameters' uncertainty ranges are relatively narrow and they contribute little to the uncertainty in  $[Cl_{2(g)}]_{peak}$ .

## 3.2.7. Kinetic salt effect

There is no significant correlation between  $[\operatorname{Cl}_{2(g)}]_{peak}$  and the kinetic salt effect parameter  $(\Psi)$  for any of the three  $[\operatorname{CO}_{2(g)}]_0$  scenarios. This verifies that two ion reactions are not important for the production of  $\operatorname{Cl}_{2(g)}$  and means that

the results presented in this study are not affected significantly if the kinetic salt effect is excluded from MAGIC. This result also means that there is no need for concern with regard to the ionic strength in the simulations ( $\sim 5$  M) exceeding the recommended range for the kinetic salt effect expression, Eq. (6), used in MAGIC,  $I \le 0.5$  M.

## 3.3. Choice of output

In this paper, the sensitivity and uncertainty analyses use the peak  $\text{Cl}_{2(g)}$  concentration as the output of interest. However, qualitatively similar results are obtained if the  $\text{Cl}_{2(g)}$  concentration at a different time is used instead. For example, re-examining case 2 ( $[\text{CO}_{2(g)}]_0 = 10 \text{ ppmv}$ ), if the analyses are conducted 500 s after the peak  $\text{Cl}_{2(g)}$  concentration occurs in each simulation, the sensitivity coefficient for  $\gamma'$  only decreases from +0.62 to +0.55 and the uncertainty contribution only decreases from 77.5% to 76.0%. The results for the other input parameters also differ slightly, but are qualitatively similar. Therefore, the authors believe that the choice of the peak  $\text{Cl}_{2(g)}$  concentration as the output of interest (as opposed to the  $\text{Cl}_{2(g)}$  concentration at a different time) does not affect the results significantly.

#### 3.4. Different simulation conditions

The authors did not attempt to vary some potential input parameters, such as aerosol diameter and initial ozone concentration, because these variables were chosen to be specific to the experiments. In addition, the uncertainty ranges of these potential input parameters were relatively small and likely contributed little to the uncertainty in MAGIC's ability to predict  $[Cl_{2(g)}]_{peak}$ .

In this study, the authors assume initial conditions similar to the original chamber experiments. The initial ozone concentration is 1600 ppby, the mean aerosol diameter is 224 nm, the particle concentration is  $1.86 \times 10^5$ particles cm<sup>-3</sup> and the initial  $CO_{2(g)}$  concentration is either 1.5, 10 or 380 ppmv. In order to obtain a qualitative understanding of the impact of these initial conditions on Cl<sub>2(g)</sub> production, the authors conducted simulations for three additional scenarios: (1) a "low ozone" scenario in which the initial ozone concentration is reduced from 1600 ppbv to 100 ppbv (typical of an urban environment), but the other conditions are unchanged; (2) a "large aerosol" scenario in which the aerosol diameter is increased from 224 nm to 2000 nm. The total liquid volume is kept constant by reducing the aerosol particle concentration to  $2.61 \times 10^{2}$  particles cm<sup>-3</sup>, but the other conditions are unchanged; and (3) a "tropospheric" scenario in which both the initial ozone concentration is reduced to 100 ppbv, the aerosol diameter is increased to 2000 nm, the particle concentration is reduced to  $2.61 \times 10^2$  particles cm<sup>-3</sup> and the initial CO<sub>2(g)</sub> concentration is 380 ppmv.

Results for all the three additional scenarios are qualitatively similar to the results presented in Table 2. The input parameter most strongly correlated to  $[Cl_{2(g)}]_{peak}$  and that produces the most uncertainty in  $[Cl_{2(g)}]_{peak}$  is still  $\gamma'$ . The other input parameters also show similar results. However, there are some notable differences. The value of  $[Cl_{2(g)}]_{peak}$ 

is reduced by almost an order of magnitude, likely due to (1) less ozone being available for photolysis which leads to less  $OH_{(g)}$  production, (2) lower total surface area which reduces the available space for the interface reaction, or (3) a combination of both. The correlation of  $\gamma'$  to  $[Cl_{2(g)}]_{peak}$  is weaker in the "large aerosol" and "tropospheric" scenarios than in the "low ozone" and manuscript scenarios, likely due to the reduction in total surface area and hence a reduction in the importance of the surface reaction.

Other species that are important in urban environments, such as oxides of nitrogen, are not included in MAGIC because the intent was to explore the sensitivity of the specific OH-NaCl system for which interface reactions have been shown to be important. Introducing additional reactions will change the model predictions since the chemistry changes, but doing a full-scale tropospheric model is outside of the scope of the present work. The authors note that other researchers (e.g. von Glasow et al., 2002; von Glasow, 2006; Pechtl and von Glasow, 2007) have introduced chlorine chemistry into a tropospheric model and examined which chemistry is most important under different conditions by changing one or a few model input parameters at a time, von Glasow (2006) found that including the interface reaction between  $OH_{(g)}$  and  $Cl_{(aq)}^-$  in a box model simulating both a marine boundary layer and the open ocean increases  $\operatorname{Cl}_{2(g)}$  production significantly. The authors hope that demonstrating the utility of a sensitivity analysis approach such as that presented here will ultimately be used in such comprehensive lower troposphere models.

#### 4. Conclusions

The interface reaction rate, specifically the probability OH<sub>(g)</sub> will react with Cl<sub>(aq,surface)</sub> once they come in contact  $(\gamma')$ , is the input parameter most strongly correlated with [Cl<sub>2(g)</sub>]<sub>peak</sub> and is responsible for most of the uncertainty  $(\sim 75\%)$  in  $[Cl_{2(g)}]_{peak}$ . In addition, this parameter's uncertainty range is relatively large, making it a good candidate for further study to reduce the uncertainty in the predicted  $[Cl_{2(g)}]_{peak}$ . If the uncertainty in  $\gamma'$  could be reduced from  $\pm 67\%$  to  $\pm 10\%$ , the uncertainty in  $[Cl_{2(g)}]_{peak}$  would decrease from  $\pm 35\%$  to  $\pm 25\%$ . Currently, measuring interface reaction kinetics is very difficult experimentally and achieving a 10% uncertainty in  $\gamma'$  is problematic. However, as techniques for probing such processes become further developed, achieving such precision may become possible. Two other good candidates for further study are the aqueous-phase reaction rate constant for  $Cl_{2(aq)}$  +  $OH_{(aq)}^- \to HOCl_{(aq)} + Cl_{(aq)}^-$  and the mass accommodation coefficient of OH since their uncertainty ranges are relatively large and together they are responsible for a significant amount of the uncertainty in  $[Cl_{2(g)}]_{peak}$ . For systems that with atmospherically relevant  $CO_{2(g)}$  concentrations ( $\sim$ 380 ppmv), the reaction rate constant for  $2CO_3^- + O_2 +$  $2H_2O \rightarrow 2CO_2 \cdot H_2O + 2O_2^-$  also becomes important. Narrowing the uncertainty ranges of the other input parameters examined in this paper would improve estimates of  $[Cl_{2(g)}]_{peak}$  only marginally.

A better understanding of the important mechanisms behind molecular chlorine production allows air quality modelers to simulate ozone production more precisely, especially in coastal regions where NaCl aerosols are more abundant (Knipping and Dabdub, 2003) and around alkaline dry lakes such as the Dead Sea in Israel (Matveev et al., 2001) and the Great Salt Lake in Utah (Stutz et al., 2002). In turn, this allows policy-makers to make better-informed decisions regarding control strategies.

## Acknowledgements

The authors thank Lisa Wingen, Marco Rodriguez and Xiao-Ying Yu for helping establish uncertainty ranges for some of the input parameters. This work was supported by grants from the United States National Science Foundation (CHE-0431312 and ATM-0423804).

## AppendixA. Supplementary data

Supplementary data associated with this article can be found, in the online version, at doi:10.1016/j. atmosenv.2008.04.041.

#### References

- Derwent, R., Høv, O., 1988. Application of sensitivity and uncertainty analysis techniques to a photochemical ozone model. Journal of Geophysical Research 93, 5185–5199.
- Finley, B.D., Saltzman, E.S., 2006. Measurement of  $\text{Cl}_2$  in coastal urban air. Geophysical Research Letters 33, L11809.
- Fitzgerald, J.W., 1991. Marine aerosols: a review. Atmospheric Environment 25A, 533-545.
- Foster, K.L., Plastridge, R.A., Bottenheim, J.W., Shepson, P.B., Finlayson-Pitts, B.J., Spicer, C.W., 2001. The role of Br<sub>2</sub> and BrCl in surface ozone destruction at polar sunrise. Science 291, 471–474.
- Gao, D.F., Stockwell, W.R., Milford, J.B., 1995. First-order sensitivity and uncertainty analysis for a regional-scale gas-phase chemical mechanism. Journal of Geophysical Research 100, 23153–23166.
- Gao, D.F., Stockwell, W.R., Milford, J.B., 1996. Global uncertainty analysis of a regional-scale gas-phase chemical mechanism. Journal of Geophysical Research 101, 9107–9119.
- von Glasow, R., 2006. Importance of the surface reaction  $OH + Cl^-$  on sea salt aerosol for the chemistry of the marine boundary layer a model study. Atmospheric Chemistry and Physics 6, 3571–3581.
- von Glasow, R., Crutzen, P.J., 2007. Tropospheric halogen chemistry. In: Holland, H.D., Turekian, K. (Eds.), Treatise on Geochemistry Update 1, 4.02, pp. 1–67.
- von Glasow, R., Sander, R., Bott, A., Crutzen, P.J., 2002. Modeling halogen chemistry in the marine boundary layer. 1. Cloud-free MBL. Journal of Geophysical Research 107, 4341.
- Hanna, S.R., Lu, Z.G., Frey, H.C., Wheeler, N., Vukovich, J., Arunachalam, S., Fernau, M., Hansen, D.A., 2001. Uncertainties in predicted ozone concentrations due to input uncertainties for the UAM-V photochemical grid model applied to the July 1995 OTAG domain. Atmospheric Environment 35, 891–903.
- Hu, J.H., Shi, Q., Davidovits, P., Worsnop, D.R., Zahniser, M.S., Kolb, C.E., 1995. Reactive uptake of Cl<sub>2</sub>(g) and Br<sub>2</sub>(g) by aqueous surfaces as a function of Br<sup>-</sup> and I<sup>-</sup> ion concentration: the effect of chemical reaction at the interface. Journal of Physical Chemistry 99, 8768–8776.
- Hunt, S.W., Roeselová, M., Wang, W., Wingen, L.M., Knipping, E.M., Tobias, D.J., Dabdub, D., Finlayson-Pitts, B.J., 2004. Formation of molecular bromine from the reaction of ozone with deliquesced NaBr aerosol: evidence for interface chemistry. Journal of Physical Chemistry A 108, 11559–11572.
- Keene, W.C., Maben, J.R., Pszenny, A.A.P., Galloway, J.N., 1993. Measurement technique for inorganic chlorine gases in the marine boundary-layer. Environmental Science and Technology 27, 866–874.
- Knipping, E.M., Dabdub, D., 2002. Modeling Cl<sub>2</sub> formation from aqueous NaCl particles: evidence for interfacial reactions and importance of Cl<sub>2</sub> decomposition in alkaline solution. Journal of Geophysical Research 107, 4360–4389.
- Knipping, E.M., Dabdub, D., 2003. Impact of chlorine emissions from sea-salt aerosol on coastal urban ozone. Environmental Science and Technology 37, 275–284.

- Knipping, E.M., Lakin, M.J., Foster, K.L., Jungwirth, P., Tobias, D.J., Gerber, R.B., Dabdub, D., Finlayson-Pitts, B.J., 2000. Experiments and simulations of ion-enhanced interfacial chemistry on aqueous NaCl aerosols. Science 288, 301–306
- Laskin, A., Wang, H., Robertson, W.H., Cowin, J.P., Ezell, M.J., Finlayson-Pitts, B.J., 2006. A new approach to determining gasparticle reaction probabilities and application to the heterogeneous reaction of deliquesced sodium chloride particles with gas-phase hydroxyl radicals. Journal of Physical Chemistry A 110, 10619–10627.
- Matveev, V., Peleg, M., Rosen, D., Tov-Alper, D.S., Hebestreit, K., Stutz, J., Platt, U., Blake, D., Luria, M., 2001. Bromine oxide–ozone interaction over the Dead Sea. Journal of Geophysical Research 106, 10375–10387.
- McKay, M.D., Beckman, R.J., Conover, W.J., 1979. Comparison of three methods for selecting values of input variables in the analysis of output from a computer code. Technometrics 21, 239–245.
- Newberg, J.T., Matthew, B.M., Anastasio, C., 2005. Chloride and bromide depletions in sea-salt particles over the northeastern Pacific Ocean. Journal of Geophysical Research 110, D06209.
- Oum, K.W., Lakin, M.J., DeHaan, D.O., Brauers, T., Finlayson-Pitts, B.J., 1998. Formation of molecular chlorine from the photolysis of ozone and aqueous sea-salt particles. Science 279, 74–77.
- Pechtl, S., von Glasow, R., 2007. Reactive chlorine in the marine boundary layer in the outflow of polluted continental air: a model study. Geophysical Research Letters 34, L11813.
- Perlmutter-Hayman, B., 1971. The primary kinetic salt effect in aqueous solution. Progress in Reaction Kinetics 6, 239–267.
- Pethybridge, A.D., Prue, J.E., 1972. Kinetic salt effects and the specific influence of ions on rate constants. Progress in Inorganic Chemistry 17, 327–390.
- Phenix, B.D., Dinaro, J.L., Tatang, M.A., Tester, J.W., Howard, J.B., McRae, G.J., 1998. Incorporation of parametric uncertainty into complex kinetic mechanisms: application to hydrogen oxidation in supercritical water. Combustion and Flame 112, 132–146.
- Pszenny, A.A.P., Keene, W.C., Jacob, D.J., Fan, S., Maben, J.R., Zetwo, M.P., Springeryoung, M., Galloway, J.N., 1993. Evidence of inorganic chlorine gases other than hydrogen chloride in marine surface air. Geophysical Research Letters 20, 699–702.
- Rochester, C.H., 1971. Salt and medium effects on reaction rates in concentrated solutions of acids and bases. Progress in Reaction Kinetics 6, 143–192.
- Rodriguez, M.A., Dabdub, D., 2003. Monte Carlo uncertainty and sensitivity analysis of the CACM chemical mechanism. Journal of Geophysical Research 108, 4443–4451.
- Sander, R., 2007. Tropospheric Measurements of Gas-phase and Aerosol Chemistry in Polar Regions. Available from: http://www.atmos-chem-phys-discuss.net/7/4285/2007/acpd-7-4285-2007-supplement.pdf Supplemental Material to Simpson et al., 2007 (cited in this work).
- Sander, S.P., Friedl, R.R., Ravishankara, A.R., Golden, D.M., Kolb, C.E., Kurylo, M.J., Molina, M.J., Moortgat, G.K., Keller-Rudek, H., Finlayson-Pitts, B.J., Wine, P.H., Huie, R.E., Orkin, V.L., 2006. Chemical kinetics and photochemical data for use in atmospheric studies. Evaluation Number 15. JPL Publication 06-2.
- Schwartz, S.E., 1986. Mass-transport considerations pertinent to aqueous phase reactions of gases in liquid-water clouds. In: Jaeschke, W. (Ed.), Chemistry of Multiphase Atmospheric Systems. NATO ASI Series, vol. G6, pp. 415–471.
- Simpson, W.R., von Glasow, R., Riedel, K., Anderson, P., Ariya, P., Bottenheim, J., Burrows, J., Carpenter, L., Frieß, U., Goodsite, M.E., Heard, D., Hutterli, M., Jacobi, H.-W., Kaleschke, L., Neff, B., Plane, J., Platt, U., Richter, A., Roscoe, H., Sander, R., Shepson, P., Sodeau, J., Steffen, A., Wagner, T., Wolff, E., 2007. Halogens and their role in polar boundary-layer ozone depletion. Atmospheric Chemistry and Physics Discussions 7, 4285–4403.
- Spicer, C.W., Chapman, E.G., Finlayson-Pitts, B.J., Plastridge, R.A., Hubbe, J.M., Fast, J.D., Berkowitz, C.M., 1998. Unexpectedly high concentrations of molecular chlorine in coastal air. Nature 394, 353–356.
- Stutz, J., Ackermann, R., Fast, J.D., Barrie, L., 2002. Atmospheric reactive chlorine and bromine at the Great Salt Lake, Utah. Geophysical Research Letters 29, 18-1–18-4.
- Tanaka, P.L., Oldfield, S., Neece, J.D., Mullins, C.B., Allen, D.T., 2000. Anthropogenic sources of chlorine and ozone formation in urban atmospheres. Environmental Science and Technology 34, 4470–4473.
- Thomas, J.L., Jimenez-Aranda, A., Finlayson-Pitts, B.J., Dabdub, D., 2006. Gas-phase molecular halogen formation from NaCl and NaBr aerosols: when are interface reactions important? Journal of Physical Chemistry A 110, 1859–1867.
- Vuilleumier, L., Harley, R.A., Brown, N.J., 1997. First- and second-order sensitivity analysis of a photochemically reactive system (a Green's function approach). Environmental Science and Technology 31, 1206–1217.